TECHNICAL RESEARCH REPORT

Power Considerations in Acoustic Emission

by J.T. Barnett, R.B. Clough and B. Kedem

T.R. 95-42

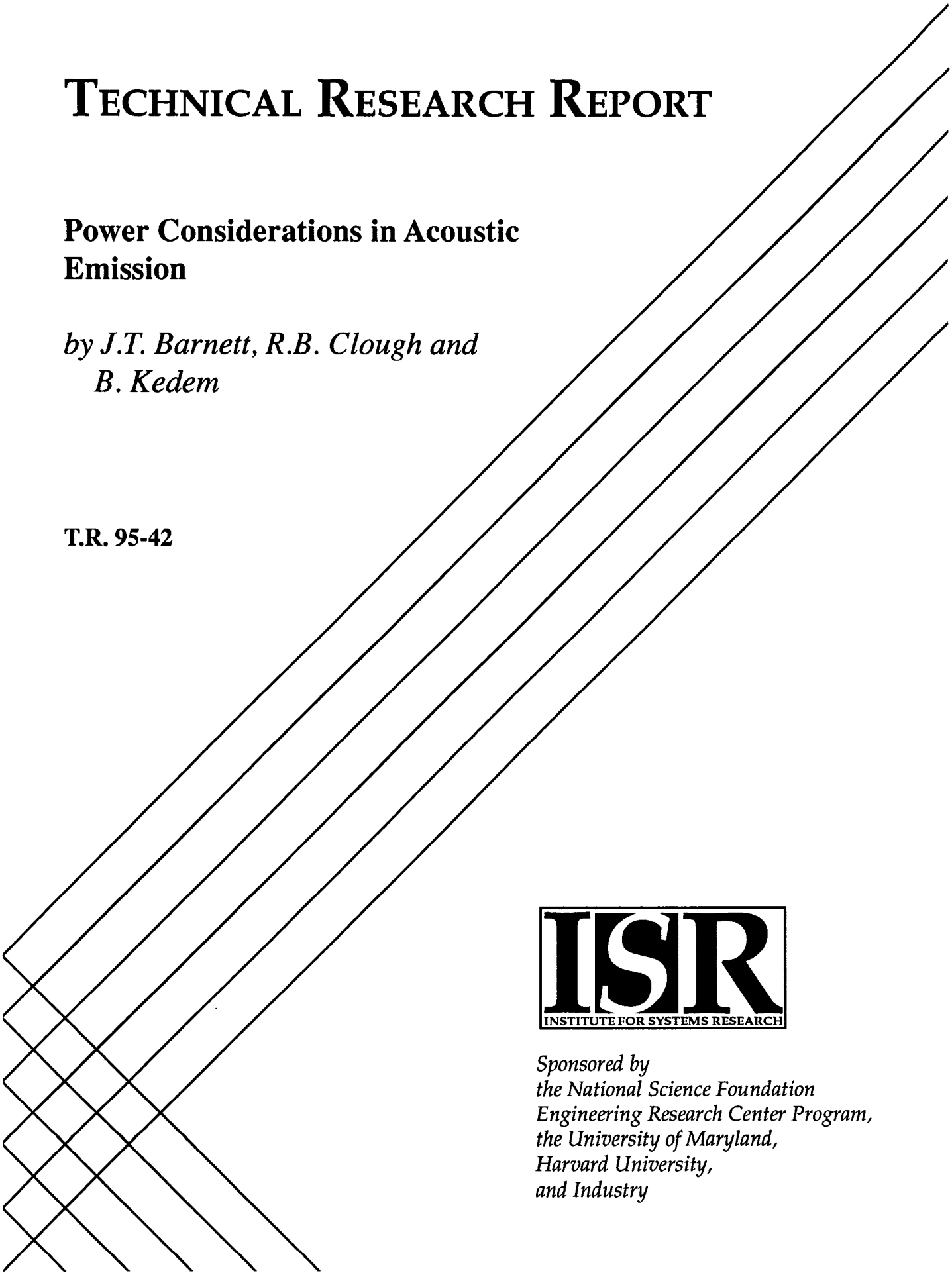

Sponsored by
the National Science Foundation
Engineering Research Center Program,
the University of Maryland,
Harvard University,
and Industry

Power Considerations in Acoustic Emission

John T. Barnett[1], Roger B. Clough[2]
and
Benjamin Kedem[1]

[1]Mathematics Department and Institute for Systems Research
University of Maryland
College Park, Maryland 20742

[2]National Institute of Science and Technology
Gaithersburg, Maryland 20899

April 1995[1]

[1]Work supported by grants AFOSR-89-0049, ONR N00014-92-C-0019, and NSF EEC-940-2384.

Abstract

In stochastic acoustic emission, both theory and experiments suggest that the power of the acoustic emission signal is proportional to the source energy . Hence, inference about the power is equivalent to inference about the source energy except for a constant multiple. In this regard, the connection between peaks exceeding a fixed level and the power in random acoustic emission waves is explored when the source energy is an impulse of short duration. Under certain conditions, the peak distribution is sensitive to power changes, determines it and is determined by it. The maximum likelihood estimator of the power from a random sample of peaks–*the peak estimator*–is more efficient than the maximum likelihood estimator–*average sum of squares*–from a random sample of the same size of signal values. When evaluated from nonrandom samples, indications are that the peak estimator may still have a relatively small mean square error. A real data example indicates that the left-truncated Rayleigh probability distribution may serve as an adequate model for high peaks.

Abbreviated Title: "Acoustic Emission"

Key words and phrases: Energy, peak distribution, Upcrossings, Maximum likelihood, Gaussian process, spectrum.

Contents

1 Introduction

In the phenomenon of acoustic emission, a burst of elastic waves is radiated into a body from a source undergoing a rapid change in stress. The acoustic emission problem consists of locating the source and characterizing it. One of the most fundamental parameters for source characterization is the power emitted, a quantity proportional to the product of the source volume and velocity. Experimentally it has been found that the detectability of such sources is given by the mechanical power density at the sensor, i.e. the elastic power of the source divided by the volume of the medium. Thus acoustic emission sources are undetectable if they are too small, move too slowly, or are diluted

in too large a body. As in electromagnetic theory, the dilution process occurs as the source elastic power flows in the direction of its acoustic Poynting vector toward neighboring regions of lower power density. This occurs along with repeated wave reflections from the outer boundaries in the process of reverberation. During this period, the waves tend to become randomized and acoustic emission can be treated as a stochastic process. In this paper we examine source characterization for such a process, beginning with a physical model of such a vibratory system adopted from seismology. We also examine the accuracy of statistical tools for source energy characterization.

Some important contributions have been previously made to this problem. Although Lyon (1964) in his theory of statistical energy analysis adopted statistical methods to the problem of energy transfer between components of a vibrating system, some of his techniques may be applicable to wave motion within a single body. For example it has been suggested that during surface mode conversion, energy is exchanged between the different mode types according to statistical energy analysis. Weaver (1988) examined diffuse wave fields. These are fields of approximately constant energy which exist for certain ranges of signal duration, specimen geometry and frequency. Experimentally, others (Clough(1987, 1992), Muravin et al. (1991)) have found that even if frequencies outside of the diffuse field range are included in the measurement (so that the total acoustic energy is measured), the energy in the sensor signal is proportional to the source energy. This being so, any estimate of the power from the sensor voltage is also an estimate of the source energy up to a constant multiple. If the proportionality constant is known by calibration, this linearity permits direct measurements of acoustic emission source energy, an example being the energy released by an advancing crack.

One of the principal features examined in this study is the relationship for such systems between power measured directly from the signal versus that obtained from the distribution of its larger peaks (truncated signal). The relationship between the *power* and *peak magnitude and its probability distribution truncated to the left*–conditional on peak magnitude greater than some threshold–is the main topic of the present paper. To gain insight as well as some generality, the underlying process is assumed to be a monotone transformation of a Gaussian stationary process. The Gaussian case is then a special case only.

Specifically, in this paper it is shown that:

1) The peak distribution, conditional on peak size greater than a fixed positive threshold L, depends on the power. Changes in the conditional peak distribution correspond to changes in power.

2) Under certain conditions, the maximum likelihood estimator of the power from a random sample $X_1, ..., X_n$ of peak heights greater than a relatively large $L > 0$,

$$\hat{\sigma^2} = \frac{\sum_{i=1}^{n} X_i^2 - nL^2}{2n}$$

is more efficient than the more direct estimator obtained from the sum of squares of a random sample $Z_1, ..., Z_n$ of signal values,

$$\tilde{\sigma^2} = \frac{\sum_{i=1}^{n} Z_i^2}{n}$$

3) When $\hat{\sigma^2}$ and $\tilde{\sigma^2}$ are computed from a time series (i.e. not a random sample), computer simulations indicate that there are levels L for which $\hat{\sigma^2}$ tends to have a smaller mean square error (MSE) than $\tilde{\sigma^2}$.

4) The conditional peak distribution of any process obtained via a monotone transformation of a stationary Gaussian process, constitutes a one parameter exponential family which generalizes the Rayleigh distribution.

5) Power is a feature useful in detecting changes in the source or in the medium.

2 Preliminaries

The existence of a basic linear relationship between source energy and average power in the sensor signal was discussed above. This is what triggered the present investigation.

2.1 An Energy Model

Experimental results show that when an energy impulse of short duration τ, say, operates on a metal plate, the expected energy density $\mathcal{E}(t)$ in the plate

rises sharply throughout the period $(0, \tau]$, and then dissipates gradually for $t > \tau$. The latter period is referred to as *ringdown* or *reverberation.* A basic physical model which describes this behavior runs as follows (e.g. see Wood (1966), pp. 536-8). For simplicity we assume that the energy impulse is of constant intensity $\mathcal{P}_s$ in $(0, \tau]$. Let $m > 0$, be an absorption constant which depends on the geometry and material of the specimen. Then, as in Clough (1987), for $0 < t \leq \tau$ and with $\mathcal{E}(0) = 0$, the time derivative is

$$\mathcal{E}'(t) = \mathcal{P}_s m \mathcal{E}(t)$$

so that the expected energy density increases as

$$\mathcal{E}(t) = \frac{\mathcal{P}_s}{m}(1 - \exp(-mt)), \quad 0 < t \leq \tau \tag{1}$$

Since the source ceases operating for $t > \tau$ we have

$$\mathcal{E}'(t) = -m\mathcal{E}(t)$$

and because now $\mathcal{E}(\tau) = \mathcal{P}_s(1 - \exp(-m\tau))/m$, we obtain for the ringdown period the solution

$$\mathcal{E}(t) = \frac{\mathcal{P}_s}{m}(1 - \exp(-m\tau))\exp(-m(t - \tau)), \quad t > \tau \tag{2}$$

Now fixing arbitrary time points $t_1, t_2 > \tau$, we observe that the power over $[t_1, t_2]$ is given by

$$\frac{1}{t_2 - t_1}\int_{t_1}^{t_2} \mathcal{E}(t)dt = \left\{\frac{C(m, \tau)}{m(t_2 - t_1)}(\exp(-mt_1) - \exp(-mt_2))\right\}\mathcal{P}_s$$

where $C(m, \tau)$ is a constant depending only on m and τ. *It follows that the source energy is proportional to the power over* $[t_1, t_2]$ *for any* $t_1 < t_2$. Moreover, we can choose a sufficiently small interval $[t_1, t_2]$ for which the mechanical vibration is approximately stationary.

Note that we have not yet touched on the observed electrical signal. This is done next.

2.2 A Statistical Vibration Model

The mechanical vibration at a location on the plate is closely related to the vibration at other locations. In other words, a time series representing the vibration at a certain location as a function of time depends on similar series observed at other locations. If we assume that the different time series–their number can be very large–are related to each other linearly, their mutual interdependence may be approximated by a first order linear system of differential equations. Thus, from a purely mathematical point of view, an idealized model which suits our purpose has the form

$$\frac{d\mathbf{y}(t)}{dt} = \mathbf{A}\mathbf{y}(t) + \mathbf{b}\delta(t) \tag{3}$$

with the initial condition $\mathbf{y}(0-) = \mathbf{0}$. Here the displacement $\mathbf{y}(t)$ is an $k \times 1$ column vector and $\mathbf{A}$ is a real square matrix of degree $k \times k$. Bolt and Brillinger (1979) and Brillinger (1987) note that (3) serves as an adequate model for a great variety of vibratory motions.

The general solution of (3) is (Boyce and DiPrima (1986), Ch. 7, Coddington and Levinson (1955), p. 78),

$$\mathbf{y}(t) = e^{\mathbf{A}t}\mathbf{0} + \mathbf{b}\int_{0-}^{t} e^{\mathbf{A}(t-s)}\delta(s)ds = e^{\mathbf{A}t}\mathbf{b}, \quad t > 0 \tag{4}$$

where

$$e^{\mathbf{A}t} = \mathbf{I} + \sum_{k=1}^{\infty} \mathbf{A}^k \frac{t^k}{k!}$$

Assume the matrix $\mathbf{A}$ has n *distinct complex eigenvalues* λ_j. Then the corresponding eigenvectors (column) $\mathbf{x}_j$ are complex and are *linearly independent.* If we define the matrix

$$\mathbf{T} = (\mathbf{x}_1, \mathbf{x}_2, ..., \mathbf{x}_n)$$

then it is nonsingular. Now,

$$\begin{aligned} \mathbf{AT} &= \mathbf{A}(\mathbf{x}_1, \mathbf{x}_2, ..., \mathbf{x}_n) = (\mathbf{A}\mathbf{x}_1, \mathbf{A}\mathbf{x}_2, ..., \mathbf{A}\mathbf{x}_n) = (\lambda_1\mathbf{x}_1, \lambda_2\mathbf{x}_2, ..., \lambda_n\mathbf{x}_n) \\ &= (\mathbf{x}_1, \mathbf{x}_2, ..., \mathbf{x}_n)\mathrm{diag}(\lambda_1, \lambda_2, ..., \lambda_n) \equiv \mathbf{TD} \end{aligned}$$

so that $\mathbf{A}$ is *diagonalizable*,

$$\mathbf{T}^{-1}\mathbf{AT} = \mathbf{D}$$

or

$$\mathbf{A} = \mathbf{T}\mathbf{D}\mathbf{T}^{-1}$$

Substituting this in $e^{\mathbf{A}t}$ we obtain

$$e^{\mathbf{A}t} = \mathbf{T}\{\mathbf{I} + \sum_{k=1}^{\infty} \mathbf{D}^k \frac{t^k}{k!}\}\mathbf{T}^{-1} = \mathbf{T}e^{\mathbf{D}t}\mathbf{T}^{-1}$$

But

$$e^{\mathbf{D}t} = \mathrm{diag}(e^{\lambda_1 t}, e^{\lambda_2 t}, ..., e^{\lambda_n t})$$

and our solution (4) becomes

$$(5) \qquad \mathbf{y}(t) = e^{\mathbf{A}t}\mathbf{b} = \mathbf{T}\mathrm{diag}(e^{\lambda_1 t}, e^{\lambda_2 t}, ..., e^{\lambda_n t})\mathbf{T}^{-1}\mathbf{b} = \sum_{j=1}^{n} \alpha_j e^{\lambda_j t}\mathbf{x}_j$$

where α_j is the jth component of the vector $\mathbf{T}^{-1}\mathbf{b}$.

Now write

$$\lambda_j = -\sigma_j + i\omega_j, \qquad \mathbf{x}_j = \mathbf{a}_j + i\mathbf{b}_j$$

where the ringdown effect suggests that $\sigma_j > 0$. Then

$$e^{\lambda_j t}\mathbf{x}_j = e^{-\sigma_j t}\{\mathbf{a}_j \cos\omega_j t - \mathbf{b}_j \sin\omega_j t\} + ie^{-\sigma_j t}\{\mathbf{b}_j \cos\omega_j t + \mathbf{a}_j \sin\omega_j t\}$$

Multiplying this by (complex) α_j, it follows that each component of $\mathbf{y}(t)$, say $y(t)$, has a *real* solution of the form

$$(6) \qquad y(t) = \sum_j \rho_j e^{-\sigma_j t}\cos(\omega_j t + \varphi_j)$$

where $-\sigma_j = \Re\lambda_j$, $\omega_j = \Im\lambda_j$.

The solution (6) indicates that the time series of mechanical vibration at a point resulting from acoustic emission may be modeled for a finite K as

$$(7) \qquad y(t) = \sum_{j=1}^{K} \rho_j e^{-\sigma_j t}\cos(\omega_j t + \varphi_j) + \epsilon(t)$$

where $\{\epsilon(t)\}$ is noise (see Brillinger (1987)). Evidently (7) is conducive to explaining the ringdown effect. When the amplitudes and phases are uncorrelated, the signal to noise ratio is relatively high, and a dominant frequency

exists (see Figures 3 and 4), the expected energy in (7) follows approximately the pattern of the energy model (2). Estimation of the parameters in (7) is discussed in Bolt and Brillinger (1979).

A transducer which transforms the mechanical vibration into the observed electrical signal, acts as a linear filter on $\{y(t)\}$. Carrying our ideas a bit further, if the σ_j in (7) are sufficiently small, then the observed electrical signal over a short interval, denoted by $\{Z(t)\}$, may be taken as a mixed spectrum stationary process with mean 0 and variance σ^2 of the form (see also Rice (1944,1945))

$$Z(t) = \sum_{j=1}^{K'} A_j \cos(\omega_j t + \phi_j) + \zeta(t) \tag{8}$$

with the damping factors removed. Thus, by the mean value theorem and in light of the preceding subsection, *the variance σ^2–that is, the power of $\{Z(t)\}$–is proportional to $\mathcal{P}_s$*. The experimental results in Clough (1987,1992) support this conclusion.

2.2.1 Experimental Verification

To see whether (8) is a reasonable model for acoustic emission, we have generated acoustic emission signals in the laboratory and computed their FFT's and autocorrelations. The data and the method of generation are described next.

Acoustic emission signals were produced by releasing a 3.175 mm diameter steel ball bearing from a fixed height of 40.5 cm above a plate of 2519-T87 hardened aluminum alloy. The plate had dimensions of $2.22 \times 30.48 \times 91.44$ cm, supported at each corner by spheres. For some of the experiments a block of 2024-T351 hardened aluminum alloy with dimensions $11.43 \times 8.25 \times 8.25$ cm was placed on the plate center , with its large face down. It was coupled to the plate with ultrasonic gel.

The locations of the impact point of the ball and the transducer were along the centerline of the plate, 15 cm from each end. The acoustic emission transducer was a piezoelectric type, coupled by an ultrasonic gel to the plate and loaded with a 0.6 N steel weight to maintain reproducibility. The calibration supplied by the manufacturer showed a dominant resonant response for the transducer at 140 kHz. The transducer was coupled by a coaxial cable directly into the high-impedance input of a 12 bit digital recorder with a

preset threshold voltage for triggering the recording. Each recording of 4096 points was made with a 200 ns sampling time interval, and the recorder permitted recording points before triggering occurred. The voltages recorded typically had a maximum range of $\pm$ 2 volts, corresponding to an integer range of ± 2048.

Figures 1 and 2 show segments of typical electrical signals obtained by dropping the small ball bearing on the metal plate and also on the same plate plus a metal block *shortly before a pronounced ringdown takes place.* The qualitative appearance of the records make the stationary assumption over a short interval more credible. The corresponding averaged (over several realizations) FFT's in Figures 3 and 4 show that the data contain strong sinusoidal components in close agreement with the model (8). Figures 5 and 6 show the corresponding estimated autocorrelation functions which do not seem to decay–consistent with the presence of line spectra. This means that the statistical dependence between well separated observations does not vanish. The estimation of power under this condition can be quite tricky (e.g. see Yaglom (1987), pp. 226-7, Koopmans (1974) p. 60).

The relationship between the source and measured acoustic emission energies produced by the steel ball bearing dropped from various increasing heights onto the aluminum alloy plate is shown in Figure 7. With a sample correlation coefficient of .974, the *observed* relationship is linear to a large degree, in line with our energy model which predicts a highly linear relationship. A least squares fit of the model $Y = aX^b$ to the data gives the estimates $\hat{a} = 0.8979$ and $\hat{b} = 1.27165$. The slight curvature is associated with an energy dissipation mechanism in the plate at the impact point, since the measured rebound height is much less than that predicted by the Hertzian elastic theory of impact. This theory has been verified experimentally by Raman (1920) as well as by others. Two such mechanisms, which would also produce the observed nonlinear response, are plastic deformation in the plate or fracture of the aluminum oxide at the plate surface.

3 Power Estimation From Peak Distribution

The relevance of the probability distribution of peak magnitude (measured from level 0) in reliability studies of mechanical systems has been known for a long time (e.g. see Lin (1967) Ch. 9, Yang (1986) Ch. 8). Regarding acoustic

emission, Ono (1976) studied the peak distribution of continuous and burst-type acoustic emission signals. An argument is made there that the Rayleigh distribution serves as an adequate model for the peak magnitude observed in continuous-type acoustic emission regardless of bandwidth. The work in these references is based to a large degree on the work of Rice (1944, 1945) and the Gaussian assumption. Builo and Tripalin (1982) have demonstrated experimentally that the exponential distribution is an adequate probability distribution model for the intervals between high peaks of acoustic emission observed in low-carbon steel.

What is of interest to us is to further explore the connection between power and peak distribution *conditional* on peaks higher than a fixed positive threshold. From the preceding discussion, this enables statistical inference about the relative (i.e. up to a constant) source energy impulse. In what follows, the observed electrical signal is assumed to be a coordinatewise monotone transformation of a Gaussian process.

3.1 A Generalization of the Rayleigh Distribution

We shall derive the conditional peak distribution in monotone transformations of Gaussian processes to find the sensitivity of the distribution to changes in power. Observe that a monotone transformation of a Gaussian process is not necessarily Gaussian, a fact which makes our results somewhat more general. In what follows we always assume that the relevant spectral moments exist.

Let $\{Z(t)\}$, $-\infty < t < \infty$, $\mathrm{E}[Z(t)] = 0$, $\mathrm{Var}[Z(t)] = \sigma^2$, be a stationary Gaussian process with autocorrelation $\rho_z(t)$, assumed twice differentiable at $t = 0$. The process in (8) fulfills this assumption when the amplitudes are independent (positive) Rayleigh random variables, the phases are independent random variables uniformly distributed in $[0, 2\pi]$ independently of the amplitudes, and the noise is a zero mean continuous spectrum stationary Gaussian process independent of the amplitudes and the phases. Consider the memoryless transformation of Z(t),

$$Y(t) = \varphi(Z(t))$$

where $\varphi(x)$ is strictly monotone increasing and continuously differentiable.

Observe that σ^2 is the power of $\{Z(t)\}$, while that of $\{Y(t)\}$ can be approximated roughly from a Taylor's series expansion to one term,

$$\mathrm{Var}[Y(t)] \approx (\varphi'(0))^2\sigma^2$$

A much more refined approximation obtained at the price of higher derivatives is obtained from Houdré and Kagan (1992). Let $X \sim \mathcal{N}(0,\sigma^2)$, and $\varphi(x)$ be a complex-valued $2n$ times differentiable function such that

$$\mathrm{E}|\varphi^{(k)}(X)|^2 < \infty, \qquad k = 0,1,\cdots,2n, \quad n \geq 1$$

Then the Houdré-Kagan inequality states that

$$\sum_{k=1}^{2n} \frac{(-1)^{k+1}}{k!}(\sigma^2)^k \mathrm{E}|\varphi^{(k)}(X)|^2 \leq \mathrm{Var}[\varphi(X)] \leq \sum_{k=1}^{2n-1} \frac{(-1)^{k+1}}{k!}(\sigma^2)^k \mathrm{E}|\varphi^{(k)}(X)|^2$$

By some integration, the joint probability density of $(Y(t), Y'(t))$, $g(u,v)$, is given by (Orsingher (1979)),

$$(9) \qquad g(u,v) = \frac{\exp\left\{\frac{1}{2\sigma^2}\left[(\varphi^{-1}(u))^2 + \frac{v^2}{(-\rho_z''(0))[\varphi'(\varphi^{-1}(u))]^2}\right]\right\}}{2\pi\sigma^2\sqrt{-\rho_z''(0)}[\varphi'(\varphi^{-1}(u))]^2}$$

$u > \varphi(-\infty), -\infty < v < \infty$. Following Rice (1944, 1945), the expected rate–per unit time–of upcrossings of level u for $\{Y(t)\}$, denoted by $N_y(u)$, is then the integral (Orsingher (1979))

$$(10) \quad N_y(u) = \int_0^\infty v g(u,v)dv = \frac{1}{2\pi}\sqrt{-\rho_z''(0)}\exp\left\{\frac{1}{2\sigma^2}[\varphi^{-1}(u)]^2\right\}$$

where $u > \varphi(-\infty)$. Related formulas both in discrete and continuous time are discussed in Barnett and Kedem (1991), and for a general discussion see Kedem (1994), Ch. 4.

By a peak we shall mean a local positive maximum observed in $\{Y(t)\}$. Note that, in a given time interval, the number of peaks located above a sufficiently high threshold level $L(>0)$ is equal to the number of upcrossings of L under the condition that there are no troughs above L. This simple fact enables us to derive the probability distribution of large peaks from (10).

Denote by the random variable X the magnitude of a peak observed in $\{Y(t)\}$. From now on we assume that L is a sufficiently large positive

constant so that the probability of a trough above L is negligible. Then from (10)

$$P(x < X \leq x + dx | X > L) = \frac{N_y(x) - N_y(x + dx)}{N_y(L)} = \frac{-N_y'(x)dx}{N_y(L)}$$

from which we obtain the conditional density of X given that $X > L$ as

$$(11)\ \mathrm{p}(x, \sigma) = \frac{1}{\sigma^2} \frac{\varphi^{-1}(x)}{\varphi'(\varphi^{-1}(x))} \exp\left\{\frac{-1}{2\sigma^2}[(\varphi^{-1}(x))^2 - (\varphi^{-1}(L))^2]\right\},\ x > L$$

We can see that (11) defines a one parameter exponential family in σ for any given monotone $\varphi(x)$ and fixed $L > 0$, the sufficient statistic being $(\varphi^{-1}(X))^2$. For $\varphi(x) = x$ and $L = 0$, $p(x, \sigma)$ reduces to the well known Rayleigh probability density function (pdf),

$$(12) \qquad p(x, \sigma) = \frac{x}{\sigma^2} \exp\left\{\frac{-x}{2\sigma^2}\right\},\ x > 0$$

Evidently, (11) provides a generalization of the Rayleigh distribution.

To illustrate how changes in the parameter σ change the general pdf $p(x, \sigma)$ in (11), we have plotted $p(x, \sigma)$ in Figures 8 to 13 using various monotone transformations and different levels L. The transformations are $\varphi(x) = x, x^3, \exp(x), 1/(1+\exp(-x)), \arctan(x)$. *We can see from the figures that the conditional peak distribution is fairly sensitive to changes in σ–a fact which might suggest σ or σ^2 as a classification feature in characterizing acoustic emission types.* Some evidence supporting this is derived from the acoustic emission data (ball dropping) described earlier. Thus from 9 independent realizations of "plate" only and then from 10 independent realizations of "plate+block" we obtain the sample variances (normalized) as depicted in Table 1. The acoustic emission variance (power) for "plate+block" tends to be appreciably lower. Crude 95% confidence intervals for "plate" and "plate+block" power are $(0.608, 0.913)$ and $(0.317, 0.523)$, respectively. The intervals do not intersect.

It is useful to note that the mean and variance of the sufficient statistic $(\varphi^{-1}(X))^2$ are readily available once $p(x, \sigma)$ is reparametrized using $\eta = -1/2\sigma^2$. Then we obtain the one parameter exponential family in natural form (Bickel and Doksum (1977), pp. 70-71),

$$p(x, \sigma) = \exp\left\{\eta(\varphi^{-1}(x))^2 + \log(-2\eta) - \eta(\varphi^{-1}(L))^2 + \log[\frac{\varphi^{-1}(x)}{\varphi'(\varphi^{-1}(x))}\right\}$$

With

$$d_0(\eta) \equiv \log(-2\eta) - \eta(\varphi^{-1}(L))^2$$

we have

$$\mathrm{E}_\eta[(\varphi^{-1}(X))^2] = -d_0'(\eta) = 2\sigma^2 + (\varphi^{-1}(L))^2 \tag{13}$$

and

$$\mathrm{Var}_\eta[(\varphi^{-1}(X))^2] = -d_0''(\eta) = 4\sigma^4 \tag{14}$$

Since inference in exponential families is based on the sufficient statistics, the moment expressions (13) and (14) are very helpful.

Table 1. *Estimated power/10^5 for acoustic emission records obtained from "plate" and "plate+block".*

	Plate	Plate+B
	0.71528	0.45827
	0.73640	0.66554
	0.40252	0.75503
	1.10723	0.28555
	0.94713	0.37602
	0.68071	0.39467
	0.76387	0.29357
	1.01470	0.24337
	0.47773	0.37462
		0.35065
Mean	0.76062	0.41973
SD	0.23366	0.16623

3.2 Estimation of Power From Peaks

By our construction, the estimation of the power in $\{Y(t)\}$ is equivalent to the estimation of σ^2 when $\varphi(x)$ is known–an assumption we have made implicitly all along. Thus, the estimation can be carried out in several ways of which we shall single out estimation based on actual values and estimation based on peaks larger than $L(> 0)$. It is interesting to compare the estimates constructed in these two ways. As we show below, there can be an advantage in precision, and possibly in speed, in estimating power from peak heights rather than from sequential voltages.

As noted above, acoustic emission data may contain discrete spectral components so that the statistical dependence in the data never dies out when observations are separated in time. In the Gaussian case we have the further complication that the sample variance is altogether inconsistent in the presence of line spectra. Thus the power estimation problem, which ostensibly appears to be rather simple, requires some caution. For this reason, we shall first assume that one has at hand random samples of independent and identically distributed random observations from the process values and from its peaks. In source characterization and reliability studies, the scientist may

stimulate a structure to generate many independent acoustic emission records by impact or by using a laser source at a very low cost. Hence, the assumption that random samples–extracted from acoustic emission records–are available has a practical base. The random sample approach enables maximum likelihood considerations which in many cases result in efficient estimators. This also may suggest a general form–at times quite unexpected–for the estimator regardless of statistical independence.

So, for a relatively large $L(> 0)$, let $X_1, X_2, ..., X_n$ be a random sample of peaks greater than L from $\{Y(t)\}$. Then from (11) the sufficient statistic for σ is

$$T \equiv \sum_{i=1}^{n} (\varphi^{-1}(X_i))^2$$

and from (13),(14),

$$\mathrm{E}_\sigma[T] = 2n\sigma^2 + n(\varphi^{-1}(L))^2$$

and, regardless of $\varphi(x)$,

$$\mathrm{Var}_\sigma[T] = 4n\sigma^4$$

The maximum likelihood estimator (MLE) of σ^2 is obtained from the equation (Bickel and Doksum (1977), p. 102)

$$2n\sigma^2 + n(\varphi^{-1}(L))^2 = \sum_{i=1}^{n} (\varphi^{-1}(X_i))^2$$

which gives

$$\hat{\sigma^2} = \frac{\sum_{i=1}^{n} (\varphi^{-1}(X_i))^2 - n(\varphi^{-1}(L))^2}{2n} \tag{15}$$

It is easily seen that $\hat{\sigma^2}$ is unbiased and

$$\mathrm{Var}_\sigma[\hat{\sigma^2}] = \frac{\sigma^4}{n} \tag{16}$$

Moreover,

$$\sqrt{n}(\hat{\sigma^2} - \sigma^2) \xrightarrow{\mathcal{L}} \mathcal{N}(0, \sigma^4)$$

Suppose on the other hand we have a random sample of values $Y_1, Y_2, ..., Y_n$ from $\{Y(t)\}$. Then the maximum likelihood estimator of σ^2 becomes

$$\tilde{\sigma^2} = \frac{\sum_{i=1}^{n} (\varphi^{-1}(Y_i))^2}{n} \tag{17}$$

which is again unbiased, but

$$\mathrm{Var}_\sigma[\tilde{\sigma}^2] = \frac{2\sigma^4}{n} \tag{18}$$

which is twice as large as the MLE from (16). We therefore have

Theorem 3.1 *The MLE $\hat{\sigma}^2$ from a random sample of size n of peaks exceeding a positive threshold L is twice as efficient as the MLE $\tilde{\sigma}^2$ from a random sample of size n of actual process values.*

It follows that we must have twice as many actual independent process values than independent peaks to achieve the same precision.

We need to clarify the last result. Recall that we are dealing with an ideal situation where potential difficulties stemming from discrete spectral components are bypassed by sampling from *independent realizations.* Then under some conditions the power can be estimated efficiently from large peaks. However, the presence of line spectra is not necessarily a hindrance and we can still use the common sense estimator which is the average of the sum of squares from a single realization–assuming zero mean. For example, when in (8) the amplitudes are fixed (not random), the phases are uniformly and independently distributed over the spectral support $(0, 2\pi]$ (assuming the unit of time to be the sampling interval), and the noise component is ergodic and independent of the random phases, then the common sense estimator *is strongly consistent.* For discussions of this point see Houdré and Kedem (1994), Li and Kedem (1993), Kedem and Slud (1994), and Kedem (1994), Ch. 6. A clarification of this technical point is given in the enclosed appendix. Whether in this case–the fixed amplitudes case–it is more efficient to estimate the power from peaks is not at all clear (although our simulation study below clarifies this point to some degree), but one thing is certain, there are many more sample values than qualified large peaks exceeding L in a single realization, a fact which may make the use of peaks somewhat dubious. Still, the import of our finding is that it points to the connection between power and peak values, and to the advantage of peaks under some conditions. Furthermore, as we shall very soon see, the estimator (15) can be used advantageously in general regardless of statistical independence.

4 The Case of Truncated Rayleigh

We now specialize the preceding general discussion to the case of most practical interest when no transformation takes place at all–that is $\varphi(x) = x$–and the power σ^2 is estimated from large peaks in the Gaussian process $\{Z(t)\}$. That is, we assume that the observed electrical signal is stationary and Gaussian with mean zero. Then (10) becomes

$$N_y(u) = \frac{1}{2\pi}\sqrt{-\rho_z''(0)}\exp\left\{\frac{u^2}{2\sigma^2}\right\} \tag{19}$$

When the measurement level u is sufficiently high (19) is also the expected rate of peaks above level u (see Rice (1945), p. 75) and the conditional density (11) of peak magnitude X given that $X > L$ for $L > 0$ becomes

$$p(x,\sigma) = \frac{x}{\sigma^2}\exp\left\{\frac{-1}{2\sigma^2}(x^2 - L^2)\right\}, x > L \tag{20}$$

which is a (left-) *truncated Rayleigh pdf.* For $L = 0$ no truncation occurs and (20) reduces to a bona fide Rayleigh probability density. The MLE from a random sample $X_1, ..., X_n$ of peaks greater than L now has the form

$$\hat{\sigma^2} = \frac{\sum_{i=1}^n X_i^2 - nL^2}{2n} \tag{21}$$

This is the *peak estimator* from which an approximate 95% confidence interval for the power is given by

$$\sigma^2 = \hat{\sigma^2} \pm 1.96\frac{\hat{\sigma^2}}{\sqrt{n}} \tag{22}$$

When instead of peaks we have a random sample of process values $Z_1, ..., Z_n$, the MLE is

$$\tilde{\sigma^2} = \frac{\sum_{i=1}^n Z_i^2}{n} \tag{23}$$

In this case the approximate 95% confidence interval is longer,

$$\sigma^2 = \tilde{\sigma^2} \pm 1.96\sqrt{\frac{2}{n}}\tilde{\sigma^2} \tag{24}$$

Since σ^2 is proportional to $\mathcal{P}_s$, from a single calibration which determines the proportionality constant we can get–using either (22) or (24)–a confidence interval for $\mathcal{P}_s$.

4.1 Plate Data Example: Large Peaks Are Rayleigh

To see whether (20) is a reasonable model for acoustic emission signals, the truncated density was fitted to the data from our plate experiment (plate only) described in Section 2.2. One may argue that high peaks are roughly nearly independent and we have used all the peaks greater than $L = 400$ from 9 independent electrical signals. The results of a chi-square goodness of fit test are given in Table 2. The results are insignificant at level .05, that is, the hypothesis that the peak data follow a truncated Rayleigh with $L = 400$ is accepted at the .05 level.

On the other hand, lowering L may give significance. Thus, with $L = 300$ and an additional category, $300 < X < 400$, we have a large observed $\hat{\chi}^2$ value as indicated in Table 3.

Table 2. *Observed versus expected frequencies under the truncated Rayleigh hypothesis with* $L = 400$. *The hypothesis is accepted at level .05.*

Category	Observed	Expected
$400 < X < 500$	40	28.93
$500 < X < 600$	23	24.87
$600 < X < 700$	12	19.26
$700 < X < 800$	13	13.58
$X > 800$	18	19.37

$\sigma^2 = 1.41 \times 10^5$

$\hat{\chi}^2 = 7.2$

d.f=3

$\chi^2_{.05} = 7.8$

Table 3. *Observed versus expected frequencies under the truncated Rayleigh hypothesis with* $L = 300$. *The hypothesis is rejected at level .05.*

Category	Observed	Expected
$300 < X < 400$	83	53.44
$400 < X < 500$	40	47.14
$500 < X < 600$	23	35.97
$600 < X < 700$	12	24.16
$700 < X < 800$	13	14.41
$X > 800$	18	13.88

$\sigma^2 = 1.05 \times 10^5$

$\hat{\chi}^2 = 29.6$

d.f=4

$\chi^2_{.05} = 9.48$

We conclude that the truncated Rayleigh model (20) with a "large" L is a reasonable model for our acoustic emission signals. Note that assuming a truncated Rayleigh model for the peaks is weaker than the full-fledged Gaussian assumption.

As for the peak estimator (21), a sample of 30 peak values above $L = 750$ from the plate data gives $\hat{\sigma}^2 = 1.01790 \times 10^5$, which is in agreement with some of the higher values in the "Plate" column in Table 1. The peaks larger than $L = 650$ from a single ball dropping are $992, 656, 768, 704, 672, 672, 800$ and $\hat{\sigma}^2 = 0.77536 \times 10^5$, a figure close to the average of the sample variances in the "Plate" column in Table 1. However, the samples here are not exactly random, and their size is too small for a meaningful comparison with the estimates in Table 1 obtained from thousands of data points. More definite conclusions may be reached from simulations under controlled conditions as in the next subsection.

4.2 Comparison Between $\hat{\sigma}^2$ and $\tilde{\sigma}^2$

4.2.1 Random Samples

Consider the stationary Gaussian autoregressive process of order two, $AR(2)$,

$$Z_t = \phi_1 Z_{t-1} + \phi_2 Z_{t-2} + \epsilon_t$$

where $t = \pm 1, \pm 2, ...$, and the ϵ_t are independent $\mathcal{N}(0,1)$. We have simulated time series of length 10,000 from the process for various choices of ϕ_1, ϕ_2. From each stretch of 100 points–there are 100 stretches–we selected one process value and one peak greater than a fixed L. The samples obtained in this way are close to being random samples since the autocorrelation decays exponentially fast and the process is Gaussian.

For $(\phi_1, \phi_2) = (0.7, -0.5)$, the true variance of the process is $\sigma^2 = 1.70455$. Table 4 shows the results of 15 independent time series of length 10,000 each from the process, each giving rise to values of $\hat{\sigma}^2$, with $L = 2$, and $\tilde{\sigma}^2$. The average, sample variance, and mean square error (MSE) from 15 values show that the peak estimator $\hat{\sigma}^2$ outperforms the average sum of squares $\tilde{\sigma}^2$. It is interesting to note that the MSE for $\hat{\sigma}^2$ is about one half of that of $\tilde{\sigma}^2$, in agreement with the theory.

Table 4. *Values of* $(\tilde{\sigma}^2, \hat{\sigma}^2)$ *corresponding to* $(\phi_1, \phi_2) = (0.7, -0.5)$, $L = 2$, $n = 100$. *The true power is* $\sigma^2 = 1.7045$.

	$\tilde{\sigma}^2$	$\hat{\sigma}^2$
	1.60930	1.74627
	1.32313	1.69699
	1.48443	1.57510
	2.00502	1.84070
	1.50617	1.61886
	1.74592	1.47999
	1.34961	1.56067
	1.56412	1.73637
	1.53982	1.60481
	1.56688	1.47263
	1.47726	1.77821
	1.43776	1.62170
	1.73009	1.72299
	1.78605	1.98918
	1.57093	1.61198
Average	1.57977	1.67043
Variance	0.03147	0.01893
MSE	0.04704	0.02010

The same experiment was repeated with 15 independent time series of

length 20,000 each from the process with $(\phi_1, \phi_2) = (0.3, -0.3)$. Here each stretch of 200 points from a given series gave us one process value and one peak above $L = 2$, so that $n = 100$. Again we can see from Table 5 a marked decrease in MSE in favor of the peak estimator.

Table 5. *Values of* $(\tilde{\sigma^2}, \hat{\sigma^2})$ *corresponding to* $(\phi_1, \phi_2) = (0.3, -0.3)$, $L = 2$, $n = 100$. *The true power is* $\sigma^2 = 1.16071$.

	$\tilde{\sigma^2}$	$\hat{\sigma^2}$
	0.94680	1.20669
	0.82511	1.09422
	1.49400	1.15819
	1.04945	1.11955
	1.10327	1.12631
	1.08123	1.14332
	1.21339	0.91157
	0.82539	1.15223
	1.01798	1.03584
	1.32814	1.07454
	0.91231	1.16006
	1.19762	1.05037
	1.04856	1.18575
	1.01346	1.01346
	1.40548	1.26507
Average	1.09748	1.11314
Variance	0.03945	0.00759
MSE	0.04345	0.00986

The preceding example was repeated for $(\phi_1, \phi_2) = (0.5, -0.5)$ but with a relatively large $L = 3$. Here not every stretch of 200 produced a peak larger than $L = 3$, so that we ended up evaluating $\hat{\sigma^2}$ from less than $n = 100$ values. However, the average sum of squares $\tilde{\sigma^2}$ was still evaluated from $n = 100$ values. The results of 20 runs are given in Table 6. The table also gives the number of qualified peaks used in the evaluation of $\hat{\sigma^2}$. Once again, the MSE of $\hat{\sigma^2}$ is smaller than the MSE of $\tilde{\sigma^2}$, despite of the fact that the peak estimator was obtained from smaller samples.

Table 6. *Values of* $(\tilde{\sigma^2}, \hat{\sigma^2})$ *corresponding to* $(\phi_1, \phi_2) = (0.5, -0.5)$, $L = 3$. *For* $\tilde{\sigma^2}$, $n = 100$. *The true power is* $\sigma^2 = 1.5$.

	$\tilde{\sigma^2}$	$\hat{\sigma^2}$	No. Peaks
	1.77575	1.55380	81
	1.64088	1.57567	77
	1.81782	1.46814	81
	1.81136	1.56932	70
	1.71470	1.41060	72
	1.26101	1.43511	71
	1.35314	1.31085	65
	1.57529	1.47282	80
	1.75162	1.35096	74
	1.86053	1.40739	77
	1.33553	1.56781	66
	1.48608	1.32215	78
	1.19041	1.25009	70
	1.41774	1.43028	77
	1.31050	1.55496	74
	1.77570	1.50617	68
	1.20113	1.57117	72
	1.68260	1.56711	74
	1.46441	1.44517	76
	1.82231	1.61418	79
Average	1.56243	1.46919	
Variance	0.05312	0.01090	
MSE	0.05702	0.01185	

The last three examples, as well as many more not reported here, support the theoretical development in that the peak estimator $\hat{\sigma^2}$ has a smaller MSE than the average sum of squares estimator $\tilde{\sigma^2}$ when the observations, process values and peak values, constitute random samples. The tendency to have a smaller MSE also has been observed more generally in time series records when the sample consists of the entire time series. This is illustrated next.

4.2.2 Non-Random Samples: Discrete Spectra

In the preceding subsection we dealt with random samples from a continuous spectrum $AR(2)$ process. In this subsection we continue to compare $\hat{\sigma^2}$ and $\tilde{\sigma^2}$ given sinusoidal data plus noise of the form (8) which is more akin to real acoustic emission.

Our sinusoidal model consists of 4 Gaussian sinusoids plus independent Gaussian noise of the form (8) where the signal to noise ratio (SNR) is $10dB$. We have generated 100 independent time series from the process each of length 1000, and evaluated $\tilde{\sigma^2}$ and $\hat{\sigma^2}$ from each series. Given a time series, $\tilde{\sigma^2}$ is evaluated from the entire record ($n = 1000$), while the peak estimator $\hat{\sigma^2}$ is obtained from all the peaks in the series greater than L. This gives 100 $\tilde{\sigma^2}$'s and 100 $\hat{\sigma^2}$'s from which we obtained an average and a sample MSE. The entire procedure was repeated 12 times. In each case we have also computed the average number of peaks used in the evaluation of the $\hat{\sigma^2}$'s. Observe that on the average, the number of qualified peaks exceeding L is much smaller than 1000.

As can be seen from Tables 7 and 8, in this particular simulation the peak estimator tends to underestimate the true power, *but still, as in random samples, it consistently gives smaller MSE.* The theory of statistics judges the overall performance of estimators by the smallness of their MSE (e.g. see Bickel and Doksum (1977), p. 117).

Table 7. *Each entry gives the average of* $\tilde{\sigma}^2$ *and* $\hat{\sigma}^2$ *and the corresponding MSE from 100 independent sinusoidal time series.* $L = 0.9$, $(\omega_1, \omega_2, \omega_3, \omega_4) = (0.8, 0.9, 1.0, 1.1)$, $SNR = 10dB$. *The true power is* $\sigma^2 = 4.3969$.

No.	$\tilde{\sigma}^2$		$\hat{\sigma}^2$		
	Ave	MSE	Ave	MSE	Ave. Peaks
1	4.42298	4.16290	4.01190	3.72059	148.010
2	4.34284	4.53365	3.91621	3.98727	148.200
3	4.41098	3.68609	3.96479	3.37266	148.170
4	4.50014	3.55210	4.01090	3.04897	151.350
5	4.35831	4.37212	3.91347	3.85721	148.030
6	4.49152	4.39982	3.99070	3.88936	151.040
7	4.33635	3.63446	3.86039	3.36573	150.130
8	4.69967	5.38226	4.20014	4.22441	150.170
9	4.44479	3.75730	4.04271	3.36434	147.660
10	4.46937	4.54787	4.00060	4.00205	149.130
11	4.39735	4.84906	3.97789	4.49687	149.030
12	4.53469	3.96519	4.10351	3.54251	149.160

Table 8. *Each entry gives the average of* $\tilde{\sigma}^2$ *and* $\hat{\sigma}^2$ *and the corresponding MSE from 100 independent sinusoidal time series.* $L = 1.3$, $(\omega_1, \omega_2, \omega_3, \omega_4) = (0.37, 0.93, 1.77, 2.53)$, $SNR = 10dB$. *The true power is* $\sigma^2 = 4.3969$.

No.	$\tilde{\sigma}^2$		$\hat{\sigma}^2$		
	Ave	MSE	Ave	MSE	Ave. Peaks
1	4.17966	3.90781	3.26522	3.75073	192.050
2	4.53908	4.34813	3.55319	3.38525	195.600
3	4.61030	3.70160	3.63241	3.01491	197.230
4	4.06742	4.15672	3.22769	4.04330	184.870
5	4.50532	2.99449	3.53389	2.69128	198.240
6	4.57901	4.35255	3.63311	3.53046	191.790
7	4.51478	4.38266	3.57757	3.65392	189.690
8	4.50253	4.17192	3.59954	3.43382	187.180
9	4.59567	4.81051	3.65653	3.52461	187.800
10	4.91599	6.33309	3.86769	4.13517	194.010
11	4.57212	4.69809	3.62599	4.02183	191.800
12	4.62566	5.45805	3.65549	4.09232	189.130

5 Summary

As discussed in the beginning of the paper, the estimation of power from noisy acoustic emission time series is important for source characterization. In this regard, we have illustrated–by deriving under assumptions a class of conditional peak distributions–the fact that relatively large peaks observed in stationary time series contain information about the power. This led to the construction of the peak estimator (21).

The power can be estimated straightforwardly by the average sum of squares–the sample variance when the mean is zero–or, alternatively, from the peak estimator (21) which uses peaks exceeding a relatively large positive threshold L. Under certain conditions, the peak estimator tends to have a smaller MSE than the average sum of squares. Simulations show that the peak estimator may underestimate the true power when the peaks do not form a random sample and/or when the peaks in the sample are not large enough. On the other hand, overestimation may occur too when the sample contains extreme peaks and L is not large enough.

Common sense suggests that *both* estimators be evaluated and used in some combination. Since under some conditions spelled out in the Appendix the average sum of squares is erratic, the peak estimator is a quantity to be reckoned with.

When troughs occur above level 0 with a high probability, the process is not narrow band to a sufficient degree and L must be relatively large. On the other hand, an excessively large L will clearly disqualify most peaks thus forcing the evaluation of the peak estimator from unduly small samples. This may result in underestimation–when the sample contains too many values close to L–or in overestimation–when the sample contains too many extreme peaks. The important question of an *optimal threshold* is open at present.

Acknowledgement. The authors are grateful to Profs. J. Dancis, T. Lee, E. Slud and P. Wolfe for very useful comments and clarifying discussions.

6 Appendix: Discrete Spectrum Consideration

To clarify the power estimation problem in mixed and discrete spectrum processes, we consider a purely discrete spectrum process. For this we follow Houdré and Kedem (1994).

Let $\{X_t\}, t = 0, \pm 1, \pm 2, \cdots$, be a weakly stationary discrete spectrum process with mean $\mathrm{E}[X_t] = m$, autocovariance $R(k) = \mathrm{E}[(X_{t+k} - m)\overline{(X_t - m)}]$, $k = 0, \pm 1, \pm 2, \cdots$, and spectral distribution $F(d\omega)$ supported at $p+1$ distinct atoms in $\{\omega_0, \omega_1, \cdots, \omega_p\} \in (-\pi, \pi]$, such that $\omega_0 = 0$. Then,

$$X_t - m = \int_{-\pi}^{\pi} e^{it\omega} \xi(d\omega)$$

where,

$$\xi(d\omega) \equiv \sum_{j=0}^{p} \xi_j \delta_{\omega_j}(d\omega), \qquad F(d\omega) = \sum_{j=0}^{p} \mathrm{E}|\xi_j|^2 \delta_{\omega_j}(d\omega)$$

and the

$$\xi(\{\omega_j\}) \equiv \xi_j$$

are orthogonal with mean zero. Clearly $\xi : \mathcal{B}(-\pi, \pi] \to L^2(P)$ is σ-additive.

As an estimator for $R(k)$ we choose the (simplified) sample autocovariance

$$\frac{1}{N} \sum_{t=1}^{N} (X_{t+k} - m)\overline{(X_t - m)}$$

The power is estimated from the average sum of squares

$$\frac{1}{N} \sum_{t=1}^{N} |X_t - m|^2$$

If we define

$$\xi^{(k)}(d\omega) \equiv \left\{ \sum_{j=0}^{p} |\xi(\{\omega_j\})|^2 e^{ik\omega_j} \right\} \delta_0(d\omega) + \sum_{j \neq l} \xi(\{\omega_j\}) \overline{\xi(\{\omega_l\})} e^{ik\omega_j} \delta_{\omega_j - \omega_l}(d\omega)$$

Then

$$(X_{t+k} - m)\overline{(X_t - m)} = \int_{-2\pi}^{2\pi} e^{it\omega} \xi^{(k)}(d\omega)$$

and we can see that for each fixed k, the lag process $(X_{t+k}-m)\overline{(X_t-m)}$ admits a Fourier representation with respect to $\xi^{(k)}:\mathcal{B}(-2\pi,2\pi]\to L^1(P)$, and a dc component

$$\xi^{(k)}(\{0\})=\sum_{j=0}^{p}|\xi(\{\omega_j\})|^2e^{ik\omega_j}$$

Theorem 6.1 *Let*

$$X_t=m+\sum_{j=0}^{p}e^{i\omega_j t}\xi_j,\qquad t=0,\pm1,\pm2,\cdots \tag{25}$$

where $E[\xi_j]=0$, *and for* $j\neq l$ $E[\xi_j\overline{\xi_l}]=0$, *be a complex valued weakly stationary process with mean* m, *autocovariance* $R(\cdot)$, *and a spectrum supported at* $p+1$ *distinct atoms* $\{\omega_0=0,\omega_1,\cdots,\omega_p\}\in(-\pi,\pi]$. *Then as* $N\to\infty$,

$$\frac{1}{N}\sum_{t=1}^{N}(X_{t+k}-m)\overline{(X_t-m)}\overset{L^1,a.s}{\to}\xi^{(k)}(\{0\}),\qquad k=0,\pm1,\pm2,\cdots \tag{26}$$

Furthermore,

$$\frac{1}{N}\sum_{t=1}^{N}(X_{t+k}-m)\overline{(X_t-m)}\overset{L^1,a.s.}{\to}R(k),\qquad k=0,\pm1,\pm2,\cdots \tag{27}$$

if and only if

$$\xi_j=\sqrt{E|\xi_j|^2}e^{i\phi_j},\qquad j=0,1,\cdots,p \tag{28}$$

where the ϕ_j *are random phases.*

The requirement of constant amplitudes $|\xi_j|$ means that if $\{X_t\}$ in (25) is a real-valued Gaussian process, its sample autocovariance is not consistent. For a proof of Theorem 6.1 and further extensions see Houdré and Kedem (1994).

7 References

1. Barnett, J. and B. Kedem (1991). Zero-crossing rates of functions of Gaussian processes, *IEEE Tr. Infor. Theory*, IT-37, pp.1188-1194.

2. Bickel, P.J. and K.A. Doksum (1977). *Mathematical Statistics, Basic Ideas and Selected Topics*, Holden-Day, Oakland, CA.

3. Bolt, B.A. and D. Brillinger (1979). Estimation of uncertainties in eigenspectral estimates from decaying geophysical time series, *Geophys. Jour. of the Royal Astronom. Soc.* , 58, pp. 593-603.

4. Boyce, W.E. and DiPrima, R.C. (1986). *Elementary Differential Equations and Boundary Value Problems*, 4'th Edition, Wiley, New York.

5. Brillinger, D.R. (1987). Fitting cosines: some procedures and some physical examples, in *Applied Probability, Stochastic Processes, and Sampling Theory*, I.B. MacNeill and G.J. Umphry (eds.), Reidel, Dordrecht, Holland, pp. 75-100.

6. Builo, S.I. and A.S. Tripalin (1982). Application of the statistical characteristics of acoustic-emission signals to measure the time rate of elementary emission events, *The Soviet Journal of Nondestructive testing* (translation of *Defektoskopiya*), 18, pp. 350-356.

7. Clough, R.B. (1987). The energetics of acoustic emission source characterization, *Materials Evaluation*, 45, pp. 556-563.

8. Clough, R.B. (1992). A scalar approach to acoustic emission, in *Int. Symp. Vibroacoustic Characterization of Materials and Structures*, P.K. Raju, Ed. ASME.

9. Coddington, E.A. and N. Levinson (1955). *Theory of Differential Equations*, McGraw-Hill, New York.

10. Houdré, C. and A. Kagan (1995). Variance inequalities for functions of Gaussian variables, *Journal of Theoretical Probability*, 8, No.1, pp. 23-30.

11. Houdré, C. and B. Kedem (1994). A note on autocovariance estimation in the presence of discrete spectra. To appear in *Statistics and Probability Letters.*

12. Kedem, B. (1994). *Time series analysis by higher order crossings*, IEEE Press, Piscataway, NJ.

13. Kedem, B. and E. Slud (1994). On autocorrelation estimation in mixed-spectrum Gaussian processes, *Stochastic Processes and Their Applications*, 49, pp. 227-244.

14. Koopmans, L.H. (1974). *Spectral Analysis of Time Series*, Academic Press, New York.

15. Li, T. and B. Kedem (1993). Strong consistency of the contraction mapping method for frequency estimation, *IEEE Tr. Infor. Theory*, 39, pp. 989-998.

16. Lin, Y.K. (1967). *Probabilistic Theory of Structural Dynamics*, McGraw-Hill, New York.

17. Lyon, R. H. (1967). Statistical analysis of power injection and response in structures and rooms, *Jour. of the Acoust. Soc. of Amer.*, 45, pp. 545-565.

18. Muravin, G.B., A.I. Merman, and L.M. Lezvinskaya (1991). Acoustic-emission method for estimating the fracture toughness of concrete in large-scale structures and buildings, *The Soviet Journal of Nondestructive testing* (translation of *Defektoskopiya*), 27, pp. 166-171.

19. Ono, K. (1976). Amplitude distribution analysis of acoustic emission signals, *Materials Evaluation*, 34, pp. 177-184.

20. Orsingher, E. (1979). Level crossings of transformations of stationary Gaussian processes, *Metron*, 37, pp. 81-100.

21. Raman, C.V. (1920). On some applications of Hertz's theory of impact, *Physical Review*, 15, pp.277-284.

22. Rice, S.O. (1944, 1945). Mathematical analysis of random noise, *Bell Syst. Tech. J.*, 23, pp. 282-332, 1944, and 24, pp. 46-156, 1945, reprinted in *Selected Papers on Noise and Stochastic Processes*," N. Wax, Ed., New York: Dover, 1954.

23. Weaver, R. (1988) Diffuse waves for materials nde, *Acousto-Ultrasonics: Theory and Applications*, J. Duke (ed.), Plenum Press, NY, pp. 35-43.

24. Wood, A. (1966). *Acoustics*, Dover Press, New York.

25. Yaglom, A.M. (1987). *Correlation Theory of Stationary and Related Random Functions*, Vol. I, Springer Verlag, New York.

26. Yang, C.Y. (1986). *Random Vibration of Structures*, Wiley-Interscience Publications, New York.

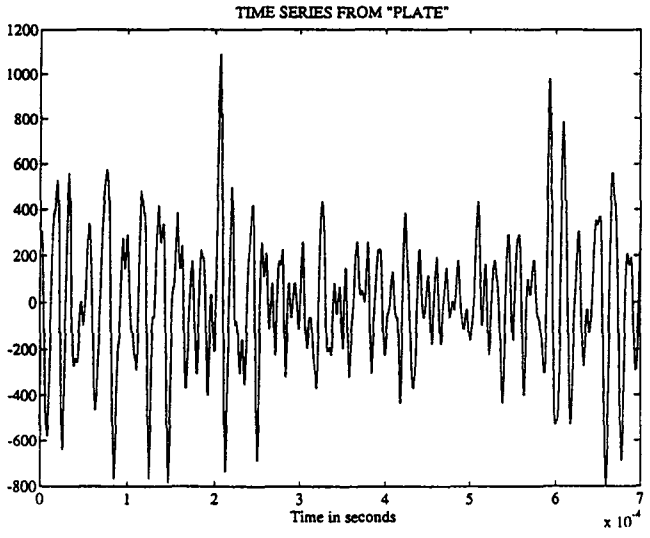

Figure 1: *An electrical signal generated by acoustic emission resulting from ball dropping on a metal plate.*

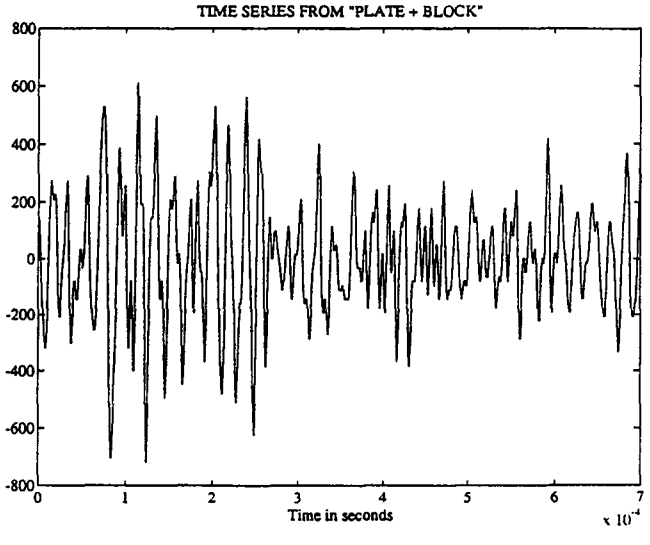

Figure 2: *An electrical signal generated by acoustic emission resulting from ball dropping on a metal plate plus block.*

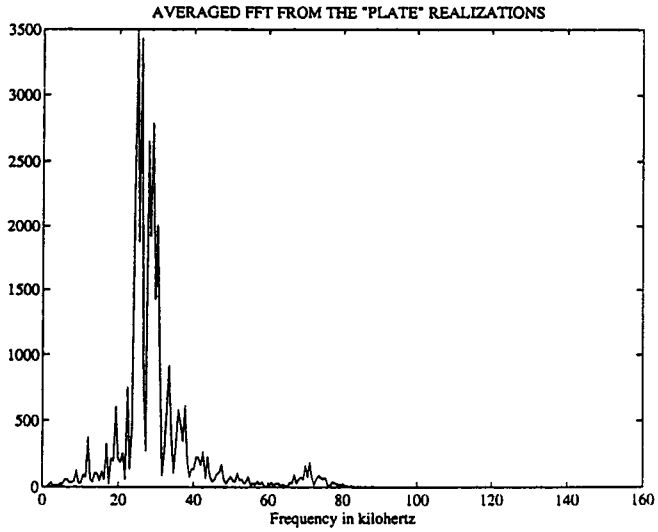

Figure 3: *A portion of average FFT from 9 independent "plate" realizations.* $n = 4096, \Delta t = 200 \times 10^{-9}$.

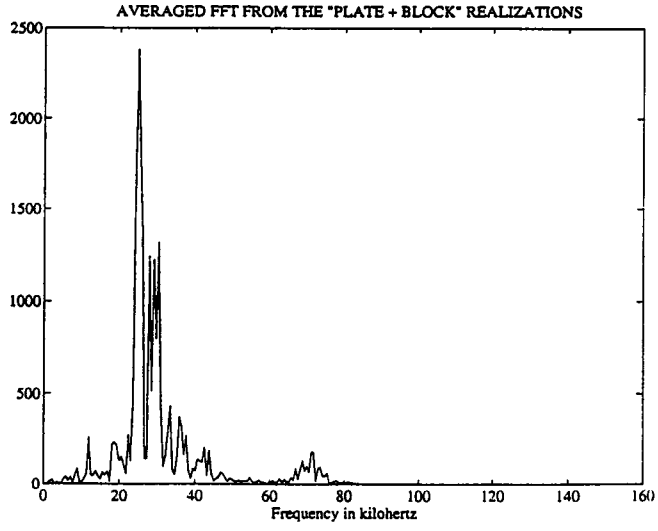

Figure 4: *A portion of average FFT from 10 independent "plate+block" realizations.* $n = 4096, \Delta t = 200 \times 10^{-9}$.

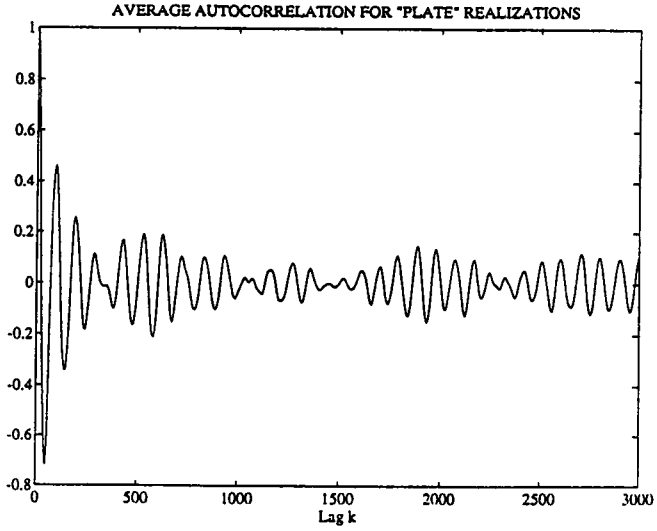

Figure 5: *Average autocorrelation from 9 independent "plate" realizations.* $n = 4096, \Delta t = 200 \times 10^{-9}$.

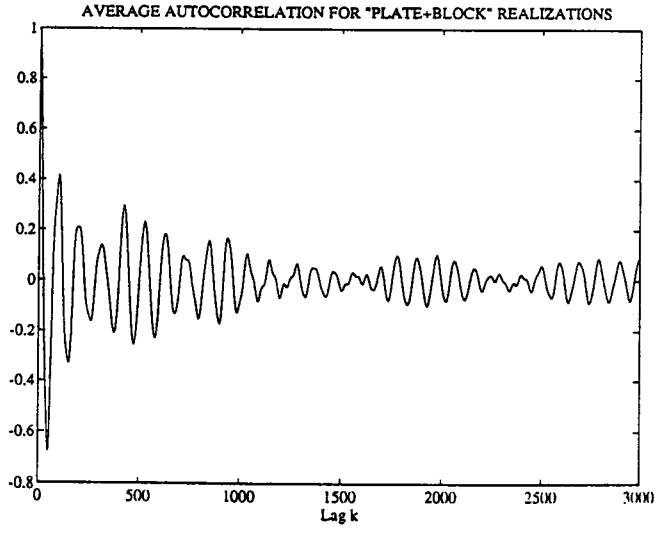

Figure 6: *Average autocorrelation from 10 independent "plate+block" realizations.* $n = 4096, \Delta t = 200 \times 10^{-9}$.

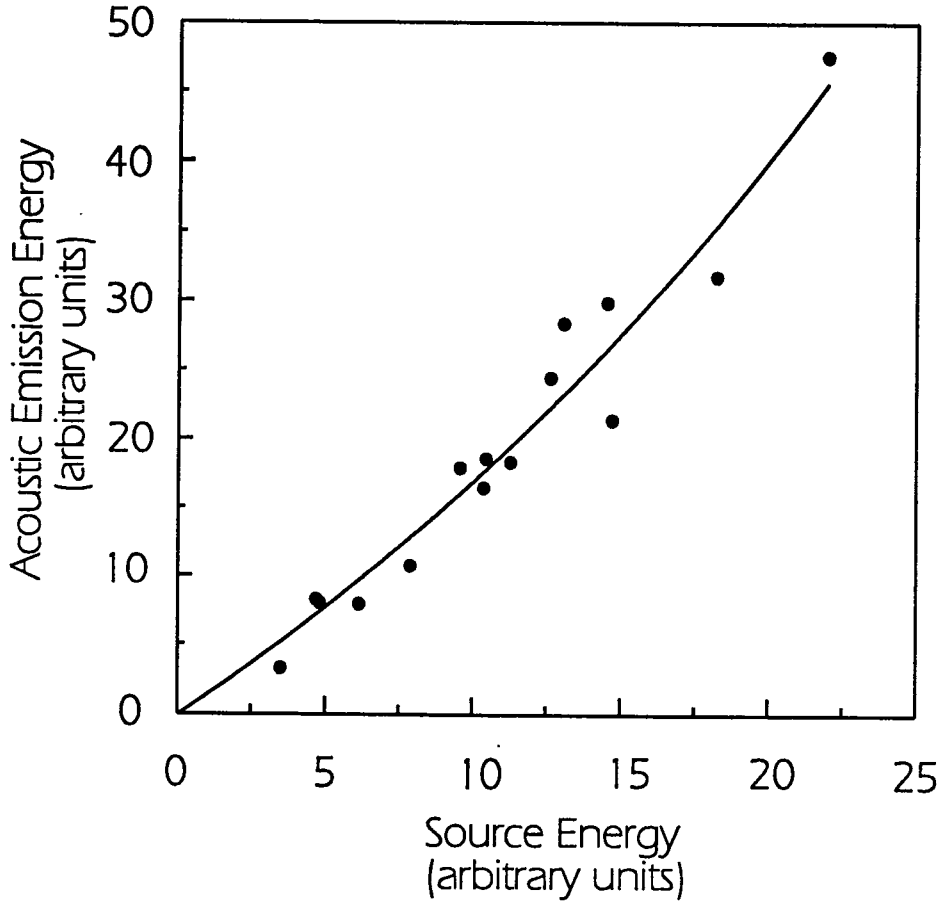

Figure 7: *Relationship between source and acoustic emission energies for a steel ball bearing dropped from various heights onto and aluminum alloy plate. The sample correlation coefficient is 0.974.*

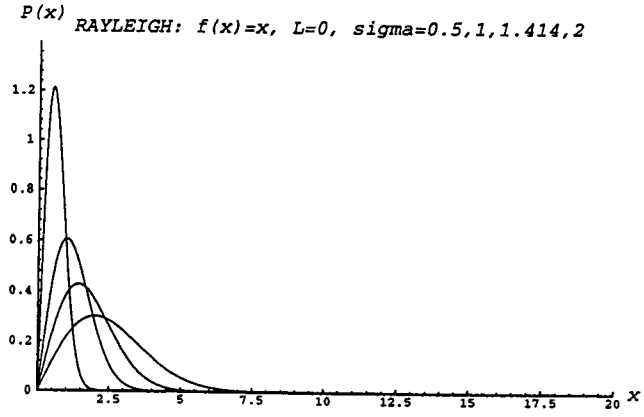

Figure 8: *Rayleigh pdf:* $p(x, \sigma)$ *with* $\varphi(x) = x, L = 0,$ *and* $\sigma = .5, 1, 1.414, 2.$

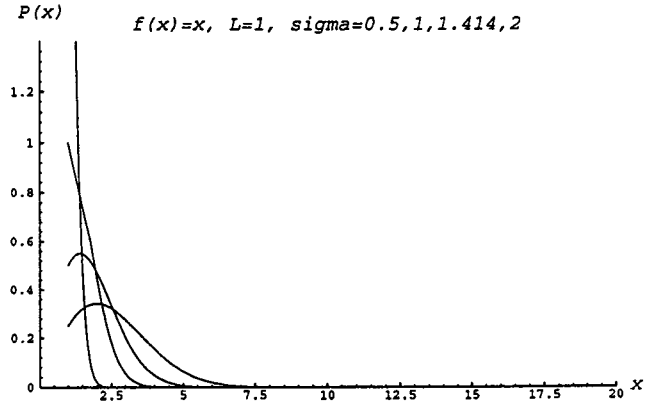

Figure 9: *Truncated Rayleigh:* $p(x, \sigma)$ *with* $\varphi(x) = x, L = 1,$ *and* $\sigma = .5, 1, 1.414, 2.$

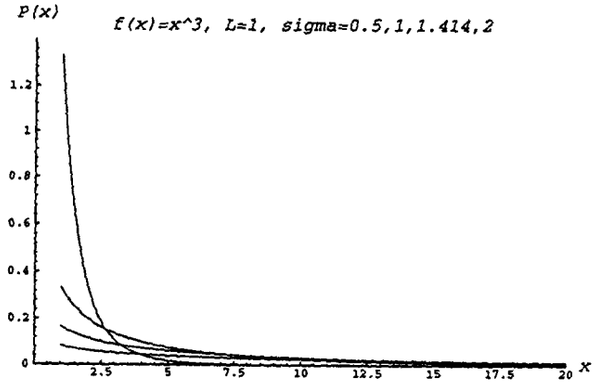

Figure 10: $p(x,\sigma)$ *with* $\varphi(x) = x^3, L = 1,$ *and* $\sigma = .5, 1, 1.414, 2.$

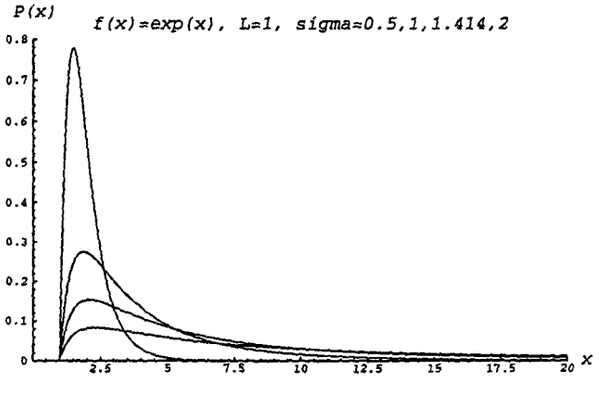

Figure 11: $p(x,\sigma)$ *with* $\varphi(x) = \exp(x), L = 1,$ *and* $\sigma = .5, 1, 1.414, 2.$

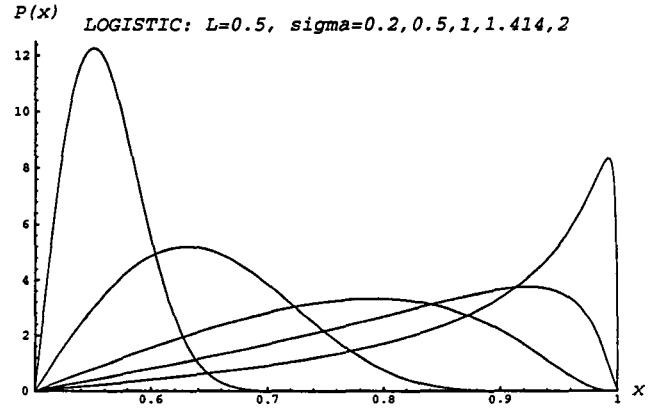

Figure 12: $p(x,\sigma)$ *with* $\varphi(x) = 1/(1+\exp(-x)), L = .5,$ *and* $\sigma = .2, .5, 1, 1.414, 2.$

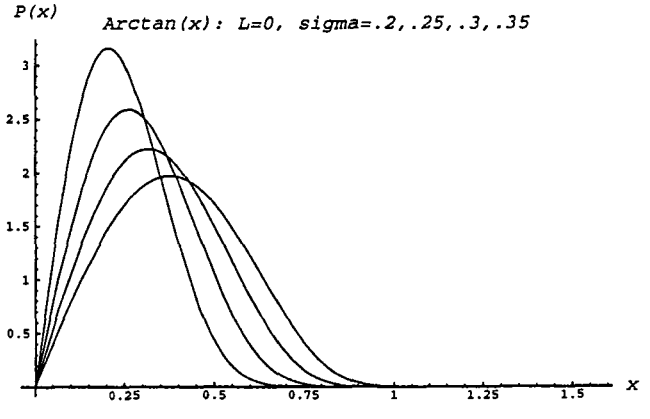

Figure 13: $p(x,\sigma)$ *with* $\varphi(x) = \arctan(x), L = 0,$ *and* $\sigma = .2, .25, .3, .35.$